HHS Public Access

Author manuscript

Bioconjug Chem. Author manuscript; available in PMC 2019 March 25.

Published in final edited form as:

Bioconjug Chem. 2018 August 15; 29(8): 2734–2740. doi:10.1021/acs.bioconjchem.8b00385.

A Dendrimer Scaffold for the Amplification of *In Vivo* Pretargeting Ligations

Brendon E. Cook[1,2,3], **Rosemery Membreno**[1,2], and **Brian M. Zeglis**[1,2,3,4,*]

[1]Department of Chemistry, Hunter College of the City University of New York, New York, NY, 10065

[2]Ph.D. Program in Chemistry, The Graduate Center of the City University of New York, New York, NY, 10016

[3]Department of Radiology, Memorial Sloan Kettering Cancer Center, New York, NY, 10065

[4]Department of Radiology, Weill Cornell Medical College, New York, NY, 10065

Abstract

The development of immunoconjugates requires a careful balance between preserving the functionality of the antibody and modifying the immunoglobulin with the desired cargo. Herein, we describe the synthesis, development, *in vivo* evaluation of a novel bifunctional dendrimeric scaffold and its application in pretargeted PET imaging. The site-specific modification of the huA33 antibody with this dendrimeric scaffold yields an immunoconjugate —^{ss}huA33-DENTCO — decorated with ~8 *trans*-cyclooctene (TCO) moieties, a marked increase compared to the ~2 TCO/mAb of a non-dendrimeric control immunoconjugate (^{ss}huA33-PEG$_{12}$-TCO). Pretargeted PET imaging and biodistribution experiments were used to compare the *in vivo* performance of these two immunoconjugates in athymic nude mice bearing subcutaneous SW1222 human colorectal cancer xenografts. To this end, the mice were administered 100 μg of each immunoconjugate followed 120 h later by the injection of a tetrazine-bearing radioligand, [^{64}Cu]Cu-SarAr-Tz. Pretargeting with ^{ss}huA33-DEN-TCO produced excellent tumoral uptake at 24 h (8.9 ± 1.9 %ID/g), more than double that created by ^{ss}huA33-PEG$_{12}$-TCO (4.1 ± 1.3 %ID/g). Critically — and somewhat surprisingly — the attachment of the G$_{0.5}$ dendrimeric structures did not hamper the *in vivo* behavior of the immunoconjugate, suggesting that this versatile bifunctional scaffold may have applications beyond pretargeting.

Graphical Abstract

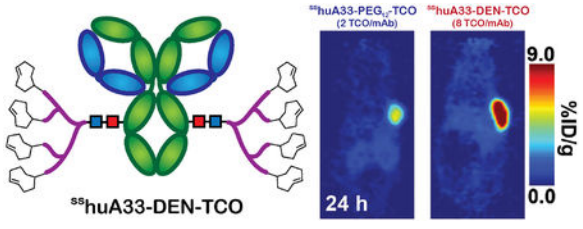

*Corresponding Author: Phone: 212-896-0443. Fax: 212-772-5332. bz102@hunter.cuny.edu.

Keywords

Positron emission tomography; colorectal carcinoma; huA33; click chemistry; bioorthogonal chemistry; inverse electron demand Diels-Alder reaction; tetrazine; *trans*-cyclooctene; strain-promoted azide-alkyne cycloaddition; pretargeting; bioconjugation; site-specific; dendrimer; dendron

INTRODUCTION

Over the past three decades, the ability of antibodies to selectivity and specifically deliver cargoes such as toxins, fluorophores, or radionuclides to sites of disease has fueled the advent of immunoconjugates in both the laboratory and the clinic. The construction of an immunoconjugate often requires a delicate balancing act between functionalizing the antibody with enough cargo molecules to facilitate the *in vivo* purpose of the final construct but not *so* many that the immunoreactivity or pharmacokinetic profile of the antibody suffer.[1] In this sense, for a given antibody, each bioconjugation reaction is a double-edged sword that simultaneously offers the reward of a more potent immunoconjugate but also the risk of a biochemically diminished vector. This is particularly true of immunoconjugates for *in vivo* pretargeting.

In vivo pretargeting is an approach to nuclear imaging and therapy that seeks to harness the tumor targeting properties of antibodies while skirting their pharmacokinetic limitations.[2, 3] To this end, *in vivo* pretargeting is predicated on decoupling the antibody and the radionuclide, injecting them separately, and allowing them to combine within the body. Our laboratory and others have previously developed an effective strategy for *in vivo* pretargeted PET imaging and therapy based on the rapid and bioorthogonal inverse electron demand Diels-Alder (IEDDA) ligation between a *trans*-cyclooctene-modified antibody (mAb-TCO) and a tetrazine (Tz)-bearing radioligand.[4–9] In pretargeted PET, the mAb-TCO construct is administered first and allowed time — typically one to five days — to accumulate at the tumor site and clear from the blood. Subsequently, the radiolabeled tetrazine is injected, whereupon it either clicks with the TCO-bearing immunoconjugate at the tumor or rapidly clears from the body (Figure 1). In this way, *in vivo* pretargeting enables the use of radionuclides that are normally incompatible with antibody-based vectors (*e.g.* ^{18}F, ^{68}Ga, ^{11}C, and ^{64}Cu), thereby facilitating imaging soon after the administration of the radiotracer and dramatically reducing radiation doses to healthy tissues compared to traditional immunoPET.[10–13]

We have recently used a chemoenzymatic bioconjugation strategy developed in our laboratory to create a site-specifically modified mAb-TCO immunoconjugate in which TCO moieties are attached to the heavy chain glycans.[14] While this construct proved effective for pretargeted PET, the modification method only allowed for the attachment of 2 TCOs per antibody due to steric hindrance within the Fc domain. It stands to reason that increasing the number TCOs on each antibody could increase the efficiency of the *in vivo* ligation — and thus uptake in the tumor — by providing more “click partners” for the Tz-bearing radioligand. Furthermore, it has been reported that TCOs can isomerize (albeit slowly) to inactive *cis*cyclooctenes *in vivo*, effectively reducing the number of reactive sites for the

radioligand.[7, 8] In light of this, increasing the number of TCOs per antibody could improve the odds of reactive isomers remaining intact following longer pretargeting intervals. This line of thought returns us to the balancing act that we discussed earlier: how we can maximize the number of TCOs while simultaneously limiting the number of bioconjugation sites? During a careful reading of the literature, one solution in particular jumped out: disulfide-core poly(amidoamine) (PAMAM) dendrimers.

Disulfide-core PAMAM dendrimers have previously been explored as platforms for the bioconjugation of drugs, radionuclides, and fluorophores to immunoglobulins.[15–17] While the loading capacity of these constructs is impressive, most — if not all — dendrimer-bearing immunoconjugates have been plagued by poor *in vivo* behavior, producing higher uptake in the liver and spleen and lower accumulation in the tumor than traditional immunoconjugates.[17–19] It is likely that these constructs underperformed because the dendrimers interfered with the ability of the antibodies to specifically and selectively bind to their molecular targets.[18, 20, 21] Nonetheless, this work provides an exciting glimpse into the potential of this approach should these limitations be overcome. Herein, we report the synthesis and development of a novel TCO-bearing scaffold based on a disulfide-core PAMAM dendrimer as well as the use of this construct to improve the performance of pretargeted PET imaging.

RESULTS AND DISCUSSION

Design

The vast majority of IEDDA-based pretargeting systems are composed of two essential elements: a TCO-bearing immunoconjugate and a Tz-based radioligand. In this investigation, we chose to employ the huA33 antibody and the [^{64}Cu]Cu-SarAr-Tz radioligand. The former is a humanized IgG_1 that targets the A33 antigen, a transmembrane glycoprotein expressed by >95% of colorectal carcinomas.[22] The latter has previously been demonstrated to exhibit rapid renal excretion as well as a favorable pharmacokinetic profile.[6] Critically, upon binding its target, huA33 remains persistent on the outside of cells, thereby facilitating the click reaction between its TCO cargo and a Tz-bearing radioligand.[22]

The final piece of the puzzle — the TCO-bearing dendrimer — will be discussed shortly. However, one last design consideration should be addressed: bioconjugation. In order to prevent the TCO-bearing dendrimer from interfering with the antibody's ability to bind its target, we have decided to employ a chemoenzymatic approach to bioconjugation developed in our laboratory (Figure 2).[14] In this approach, the antibody is first treated with EndoS, an endoglycosidase that hydrolyzes the chitobiose core of the asparagine-linked heavy chain glycans. Subsequently, the immunoconjugate is treated with a promiscuous galactosyltransferase — Gal-T(Y289L) — and an azide-modified monosaccharide — *N*-azidoacetylgalactosamine (GalNAz) — in order to incorporate azides into the residual glycan chains. The azide-bearing antibody can then be modified easily using dibenzocyclooctyne (DBCO)-bearing substrates via the strain-promoted azide-alkyne cycloaddition (SPAAC).[23, 24]

Construction of the TCO-Bearing Dendrimer

Disulfide-core PAMAM dendrimers provide a versatile, commercially-available, and hydrophilic synthetic scaffold. They can be modified on the NH_2-bearing 'branches' using amine-reactive reagents and — after reduction — on the sulfhydryl-containing 'core' with thiol-reactive moieties. In this case, we set out to modify the former with TCOs and the latter with a PEG_4-containing variant of DBCO for SPAAC. The synthesis of the TCO-bearing dendrimer was performed in three steps with an overall yield of 33% (Figure 3). The G_1 starting material was first reduced using tris(2-carboxyethyl)phosphine (TCEP) for 1 h at 25 °C. Without purification, DBCO-PEG_4-maleimide was added in molar excess, and the reaction mixture was incubated at 25 °C for 24 h to produce $G_{0.5}$-PAMAM-PEG_4-DBCO or, more simply, DBCODEN-NH_2. Following chromatographic purification, DBCO-DEN-NH_2 was incubated under basic conditions with a vast molar excess of TCO-NHS at 25 °C for 48 h. The final product — DBCO-DEN-TCO — was purified via reversed phase C_{18} HPLC. Characterization by high resolution mass spectrometry revealed that the maleimide linkage underwent hydrolysis; however it has been demonstrated in the literature that this affects neither the linkage nor the utility of the molecule.[25]

Bioconjugation

As we noted above, a chemoenzymatic strategy was used to site-specifically attach the TCO-bearing dendrimers to huA33 (Figure 2). To this end, huA33 was first treated with EndoS and then GalT(Y289L)/GalNAz in order to incorporate azides into the heavy chain glycans of the antibody, ultimately producing ^{ss}huA33-N_3. DBCO-DEN-TCO was then conjugated to ^{ss}huA33-N_3 via overnight incubation in aqueous buffer at 25°C. The final product — ^{ss}huA33-DEN-TCO — was purified via size exclusion chromatography and characterized by MALDI-ToF, which confirmed the presence of ~2.0 DEN-TCO scaffolds per mAb. This, of course, means that each ^{ss}huA33-DEN-TCO construct boasts ~8.0 TCO/mAb. The specificity of the bioconjugation was validated via SDS-PAGE, which clearly displayed a positive shift in the mass of the heavy chain but no shift in the mass of the light chain (Figure S2). As a control construct, ^{ss}huA33-DEN-NH_2 was synthesized in a similar manner using DBCO-DEN-NH_2. In this case, MALDI-ToF likewise confirmed a degree of labeling of ~2 DEN-NH_2/mAb.

The site-specifically labeled, TCO-bearing huA33 immunoconjugate that we have previously published, ^{ss}huA33-PEG_{12}-TCO, was chosen as a 'dendrimer-lacking' control immunoconjugate for the investigation.[26] The synthesis of this construct — which differs slightly from that of ^{ss}huA33-DEN-TCO — has been reported (Figure S1). Briefly, huA33 was first treated with β−1,4-galactosidase and then GalT(Y289L)/GalNAz in order to incorporate azides into the heavy chain glycans of the antibody. Unlike EndoS, β−1,4-galactosidase cleaves only the final galactose residues of the biantennary glycans, meaning this method facilitates the incorporation a total of four azides into the glycans. DBCO-PEG_{12}-TCO was then conjugated to the azide-modified antibody, creating the finished product: ^{ss}huA33-PEG_{12}-TCO. Despite the presence of four azides, MALDI-ToF analysis revealed that ^{ss}huA33-PEG_{12}-TCO had a degree of labeling of only ~2 TCO/mAb, likely due to steric hindrance within the Fc region of the antibody.

The immunoreactivity of both ^{ss}huA33-DEN-TCO and ^{ss}huA33-PEG$_{12}$-TCO were tested prior to *in vivo* studies via antigen saturation binding assays using SW1222 cells expressing the A33 antigen. In early assays, ^{ss}huA33-DEN-TCO displayed a high degree of non-specific binding to the microcentrifuge tubes, though this was soon circumvented via the use of tubes pretreated with BSA. Ultimately, the immunoreactive fractions of ^{ss}huA33-DEN-TCO and ^{ss}huA33-PEG$_{12}$-TCO were found to be 0.92 ± 0.06 and 0.97 ± 0.01, respectively.

Pretargeted PET Imaging and Biodistribution Experiments

PET imaging and biodistribution experiments were performed to explore the efficacy of *in vivo* pretargeting with ^{ss}huA33-DEN-TCO and [^{64}Cu]Cu-SarAr-Tz. To this end, athymic nude mice bearing subcutaneous SW1222 human colorectal cancer xenografts were first injected with either ^{ss}huA33-DEN-TCO or ^{ss}huA33-PEG$_{12}$-TCO (100 μg, 0.67 nmol), followed 120 h later by the administration of [^{64}Cu]Cu-SarAr-Tz (16.7 MBq; 450 μCi, 0.75 nmol). It is important to note that we used a particularly long pretargeting interval (120 h) in this investigation in order to probe if this new technology could improve the performance of the pretargeting system using long gaps between the two injections. Static PET scans were performed 4 and 24 h after the injection of the radioligand (Figure 4A). Immediately after the second set of PET scans, the two cohorts of mice were sacrificed, and their organs were harvested, rinsed, dried in open air, weighed, and assayed for radioactivity on an automated gamma counter. The differences between the *in vivo* performances of the two systems are readily apparent in both the images and the biodistribution (Figure 4B). Most notably, ^{ss}huA33-DEN-TCO produces double the tumoral activity concentration of ^{ss}huA33-PEG$_{12}$-TCO: 8.9 ± 1.9 %ID/g vs. 4.1 ± 1.3 %ID/g, respectively. Background uptake is observed in the kidneys for both groups and can be attributed to the retention of the radioligand.(*12*) At the same time, both the blood and well-perfused organs (*i.e.* heart, lungs, liver) demonstrate noticeably higher uptake in the mice administered the dendrimer-bearing immunoconjugate. The higher blood values in particular — 2.0 ± 1.0% ID/g for ^{ss}huA33-DEN-TCO compared with 0.8 ± 0.4% ID/g for ^{ss}huA33-PEG$_{12}$-TCO — led to an investigation of the serum half-lives of the two constructs (discussed below).

Tumoral Uptake of the Immunoconjugates

The promising data obtained in the pretargeting experiments prompted a second experiment to measure the tumoral uptake of the immunoconjugates alone. To this end, the two immunoconjugates — ^{ss}huA33-DEN-TCO and ^{ss}huA33-PEG$_{12}$-TCO — were non-site-specifically labeled with the bifunctional chelator *p*-SCN-Bn-desferrioxamine (DFO-NCS) in order to facilitate radiolabeling with ^{89}Zr. We selected ^{89}Zr-based imaging as means to track the constructs *in vivo* for two reasons: (1) the long half-life of ^{89}Zr ($t_{1/2}$ ~ 3.3 d) allowed us to follow the immunoconjugates over several days and (2) we wanted the TCO moieties of the immunoconjugates to remain intact throughout the experiment. Athymic nude mice bearing SW1222 xenografted tumors (n = 5) were administered 8.5 MBq (230 μCi, 100 μg) of either ^{89}Zr-DFO-labeled construct — ^{89}Zr-DFO-^{ss}huA33-DEN-TCO or ^{89}Zr-DFO-^{ss}huA33-PEG$_{12}$-TCO — via tail-vein injection. At 120 h post-injection, static PET scans were acquired, and both cohorts were then sacrificed; subsequently, their organs were harvested, rinsed, dried in open air, weighed, and assayed for radioactivity on an automated gamma counter. Both constructs exhibited excellent tumor uptake (Figure 5),

with ^{89}Zr-DFO-^{ss}huA33-DEN-TCO and ^{89}Zr-DFO-^{ss}huA33-PEG$_{12}$-TCO producing activity concentrations of 47.9 ± 14.1% ID/g and 43.8 ± 4.1% ID/g in the tumor, respectively. While the mean uptake of the ^{89}Zr-labeled dendrimer-antibody conjugate was slightly higher, the difference was not statistically significant (P>0.05). This result underscores that in the *in vivo* pretargeting experiments, the availability of ~8 TCOs/mAb on ^{ss}huA33-DEN-TCO compared to ~2 TCOs/mAb on ^{ss}huA33-PEG$_{12}$-TCO is responsible for the higher uptake of radioligand at the tumor.

Serum Clearance Pharmacokinetics

In the pretargeting experiments, ^{ss}huA33-DEN-TCO (2.0 ± 1.0 %ID/g) produced higher activity concentrations in the blood than ^{ss}huA33-PEG$_{12}$-TCO (0.8 ± 0.4 %ID/g). This suggests that the ^{ss}huA33-DEN-TCO immunoconjugate has a longer pharmacokinetic half-life in serum than ^{ss}huA33-PEG$_{12}$-TCO. This is, perhaps, not surprising in light of the relatively large dendrimeric scaffolds attached to the former. Nonetheless, a more thorough investigation was warranted. A serum half-life study was performed in an effort to explore the clearance of these immunoconjugates from the blood more quantitatively. To this end, DFO-modified variants of each construct — DFO-^{ss}huA33-DEN-TCO or DFO-^{ss}huA33-PEG$_{12}$-TCO — were again used to facilitate radiolabeling with ^{89}Zr. In addition to these two constructs, three other huA33-based immunoconjugates were modified with DFO and studied as controls: native huA33, huA33 that had been deglycosylated with EndoS (huA33-EndoS), and ^{ss}huA33-DEN-NH$_2$. Healthy female athymic nude mice (n = 5) were administered 2.2 MBq of each 89Zr-DFO-labeled radioimmunoconjugate; tail-vein blood draws were performed at 2, 6, 24, 48, 72, 120, and 144 h post-injection; and the blood from each sampling was weighed and assayed for radioactivity on a gamma-counter (Figure 6). In addition, PET images were also obtained to visualize the *in vivo* behavior of each construct (Figure S3).

The serum half-life of ^{89}Zr-DFO-^{ss}huA33-DEN-TCO ($t_{1/2}$ ~ 78 h) was dramatically longer than that of ^{89}Zr-DFO-^{ss}huA33-PEG$_{12}$-TCO ($t_{1/2}$ ~ 30 h), producing a significantly higher activity concentration in the blood at 144 h post-injection (P < 0.0005). Interestingly, the half-life of ^{89}Zr-DFO-^{ss}huA33-PEG$_{12}$-TCO was most similar to that of native huA33, while the half-life of ^{89}Zr-DFO-^{ss}huA33-DEN-TCO was far closer to that of the EndoS-deglycosylated antibody (Table S1). This suggests that in this case, the glycosylation state of the antibody has a stronger influence on the blood clearance of the antibody than the presence of the dendrimeric scaffold. Furthermore, ^{89}Zr-DFO-^{ss}huA33-DEN-NH$_2$ exhibited a similar rate of clearance to ^{89}Zr-DFO-^{ss}huA33-DEN-TCO despite differences in the charge and lipophilicity of the dendrimers attached to each construct. This result hints at the possibility that dendrimeric scaffolds bearing a wide variety of cargoes could be attached to antibodies without dramatically impairing their *in vivo* performance, though of course more study in this area is needed.

CONCLUSION

In the preceding pages, we have described the synthesis, characterization, and *in vivo* application of a bifunctional, TCO-bearing dendrimeric scaffold: DBCO-DEN-TCO. A site-

specifically modified immunoconjugate decorated with a pair of these TCO-bearing dendrimers — ^{ss}huA33-DEN-TCO — proved to be a highly effective platform for pretargeted PET imaging. Indeed, pretargeted PET and biodistribution experiments in a murine model of colorectal carcinoma revealed that ^{ss}huA33-DEN-TCO produced dramatically improved absolute tumoral activity concentrations compared to an analogous, dendrimer-lacking immunoconjugate (^{ss}huA33-PEG_{12}-TCO). The foundation of this improved performance almost certainly lies in the higher number of TCOs/mAb on ^{ss}huA33-DEN-TCO, a trait that not only provides more *in vivo* reaction partners for tetrazine radioligands but also acts as 'insurance' against the slow isomerization of *trans*-cyclooctene to *cis*-cyclooctene in the body. Moving beyond pretargeting, we also believe that this work could have more general implications for bioconjugation chemistry. More specifically, we have demonstrated that our dendrimeric scaffolds can be site-specifically attached to an antibody without impairing its ability to bind its target *in vivo*. It is important to note, however, that while this bioconjugation strategy preserves the integrity of the immunoglobulin, it also appears to increase the serum half-live of the immunoconjugate. Ultimately, it is our hope that this study has an ongoing impact not only on the study of *in vivo* pretargeting but also on the field of bioconjugation chemistry as a whole.

Supplementary Material

Refer to Web version on PubMed Central for supplementary material.

ACKNOWLEDGEMENTS

Services provided by the MSKCC Small-Animal Imaging Core Facility were supported in part by NIH grants R24 CA83084 and P30 CA08748. The authors would also like to thank the generous support of the National Institutes of Health (4R00CA178205–02 and R01CA204167; BMZ), the National Institute on Minority Health and Health Disparities (G12MD007599; BMZ), and the Tow Foundation Fellowship Program in Molecular Imaging and Nanotechnology (BEC). Finally, the authors would also like to thank Devin Cook and Luke Ketchum for fruitful discussions.

REFERENCES

(1). Zeglis BM, and Lewis JS (2011) A practical guide to the construction of radiometallated bioconjugates for positron emission tomography. Dalton Trans. 40, 6168–6195. [PubMed: 21442098]

(2). Altai M, Membreno R, Cook BE, Tolmachev V, and Zeglis BM (2017) Pretargeted imaging and therapy. J. Nucl. Med 58.

(3). Goldenberg DM, Chang CH, Rossi EA, McBride WJ, and Sharkey RM (2012) Pretargeted molecular imaging and radioimmunotherapy. Theranostics 2, 523–540. [PubMed: 22737190]

(4). Rossin R, Renart Verkerk P, van den Bosch SM, Vulders RCM, Verel I, Lub J, and Robillard MS (2010) In vivo chemistry for pretargeted tumor imaging in live mice. Angew. Chem. Int. Ed 49, 3375–3378.

(5). Zeglis BM, Sevak KK, Reiner T, Mohindra P, Carlin SD, Zanzonico P, Weissleder R, and Lewis JS (2013) A pretargeted PET imaging strategy based on bioorthogonal Diels-Alder click chemistry. J. Nucl. Med 54, 1389–96. [PubMed: 23708196]

(6). Zeglis BM, Brand C, Abdel-Atti D, Carnazza KE, Cook BE, Carlin S, Reiner T, and Lewis JS (2015) Optimization of a pretargeted strategy for the PET imaging of colorectal carcinoma via the modulation of radioligand pharmacokinetics. Mol. Pharm 12, 3575–3587. [PubMed: 26287993]

(7). Rossin R, van den Bosch SM, Ten Hoeve W, Carvelli M, Versteegen RM, Lub J, and Robillard MS (2013) Highly reactive trans-cyclooctene tags with improved stability for Diels-Alder chemistry in living systems. Bioconjug. Chem 24, 1210–7. [PubMed: 23725393]

(8). Rossin R, van Duijnhoven SM, Lappchen T, van den Bosch SM, and Robillard MS (2014) Trans-cyclooctene tag with improved properties for tumor pretargeting with the diels-alder reaction. Mol. Pharm 11, 3090–6. [PubMed: 25077373]

(9). Blackman ML, Royzen M, and Fox JM (2008) Tetrazine ligation: Fast bioconjugation based on inverse-electron-demand Diels−Alder reactivity. JACS 130, 13518–13519.

(10). Meyer J-P, Houghton JL, Kozlowski P, Abdel-Atti D, Reiner T, Pillarsetty NVK, Scholz WW, Zeglis BM, and Lewis JS (2016) 18F-based pretargeted PET imaging based on bioorthogonal Diels-Alder click chemistry. Bioconjug. Chem 27, 298–301. [PubMed: 26479967]

(11). Meyer JP, Kozlowski P, Jackson J, Cunanan KM, Adumeau P, Dilling TR, Zeglis BM, and Lewis JS (2017) Exploring structural parameters for pretargeting radioligand optimization. J. Med. Chem 60, 8201–8217. [PubMed: 28857566]

(12). Herth MM, Andersen VL, Lehel S, Madsen J, Knudsen GM, and Kristensen JL (2013) Development of a (11)C-labeled tetrazine for rapid tetrazine-trans-cyclooctene ligation. Chem. Commun 49, 3805–7.

(13). Denk C, Svatunek D, Mairinger S, Stanek J, Filip T, Matscheko D, Kuntner C, Wanek T, and Mikula H (2016) Design, synthesis, and evaluation of a low-molecular-weight 11C-labeled tetrazine for pretargeted PET imaging applying bioorthogonal in vivo click chemistry. Bioconjug. Chem 27, 1707–1712. [PubMed: 27308894]

(14). Zeglis BM, Davis CB, Aggeler R, Kang HC, Chen A, Agnew BJ, and Lewis JS (2013) Enzyme-mediated methodology for the site-specific radiolabeling of antibodies based on catalyst-free click chemistry. Bioconjug. Chem 24, 1057–1067. [PubMed: 23688208]

(15). Nwe K, Milenic DE, Ray GL, Kim Y-S, and Brechbiel MW (2012) Preparation of cystamine core dendrimer and antibody-dendrimer conjugates for MRI angiography. Mol. Pharm 9, 374–381. [PubMed: 21882823]

(16). Wu G, Barth RF, Yang W, Kawabata S, Zhang L, and Green-Church K (2006) Targeted delivery of methotrexate to epidermal growth factor receptor-positive brain tumors by means of cetuximab (IMC-C225) dendrimer bioconjugates. Mol. Cancer Ther 5, 52–9. [PubMed: 16432162]

(17). Kobayashi H, Sato N, Saga T, Nakamoto Y, Ishimori T, Toyama S, Togashi K, Konishi J, and Brechbiel MW (2000) Monoclonal antibody-dendrimer conjugates enable radiolabeling of antibody with markedly high specific activity with minimal loss of immunoreactivity. Eur. J. Nucl. Med 27, 1334–9. [PubMed: 11007515]

(18). Kobayashi H, Wu C, Kim MK, Paik CH, Carrasquillo JA, and Brechbiel MW (1999) Evaluation of the in vivo biodistribution of indium-111 and yttrium-88 labeled dendrimer-1B4M-DTPA and its conjugation with anti-Tac monoclonal antibody. Bioconjug. Chem 10, 103–11. [PubMed: 9893971]

(19). Wängler C, Moldenhauer G, Eisenhut M, Haberkorn U, and Mier W (2008) Antibody−dendrimer conjugates: The number, not the size of the dendrimers, determines the immunoreactivity. Bioconjug. Chem 19, 813–820. [PubMed: 18361514]

(20). Aghevlian S, Lu Y, Winnik MA, Hedley DW, and Reilly RM (2018) Panitumumab modified with metal-chelating polymers (MCP) complexed to 111In and 177Lu—An EGFR-targeted theranostic for pancreatic cancer. Mol. Pharm 15, 1150–1159. [PubMed: 29314858]

(21). Lu Y, Ngo Ndjock Mbong G, Liu P, Chan C, Cai Z, Weinrich D, Boyle AJ, Reilly RM, and Winnik MA (2014) Synthesis of polyglutamide-based metal-chelating polymers and their site-specific conjugation to trastuzumab for auger electron radioimmunotherapy. Biomacromolecules 15, 2027–37. [PubMed: 24838009]

(22). Ackerman ME, Chalouni C, Schmidt MM, Raman VV, Ritter G, Old LJ, Mellman I, and Wittrup KD (2008) A33 antigen displays persistent surface expression. Cancer Immunol. Immunother 57, 1017–27. [PubMed: 18236042]

(23). Meyer J-P, Adumeau P, Lewis JS, and Zeglis BM (2016) Click chemistry and radiochemistry: The first 10 years. Bioconjug. Chem 27, 2791–2807. [PubMed: 27787983]

(24). Agard NJ, Prescher JA, and Bertozzi CR (2004) A strain-promoted [3 + 2] azide−alkyne cycloaddition for covalent modification of biomolecules in living systems. JACS 126, 15046–15047.

(25). Barradas RG, Fletcher S, and Porter JD (1976) The hydrolysis of maleimide in alkaline solution. Can. J. Chem 54, 1400–1404.

(26). Cook BE, Adumeau P, Membreno R, Carnazza KE, Brand C, Reiner T, Agnew BJ, Lewis JS, and Zeglis BM (2016) Pretargeted PET imaging using a site-specifically labeled immunoconjugate. Bioconjug. Chem 27, 1789–1795. [PubMed: 27356886]

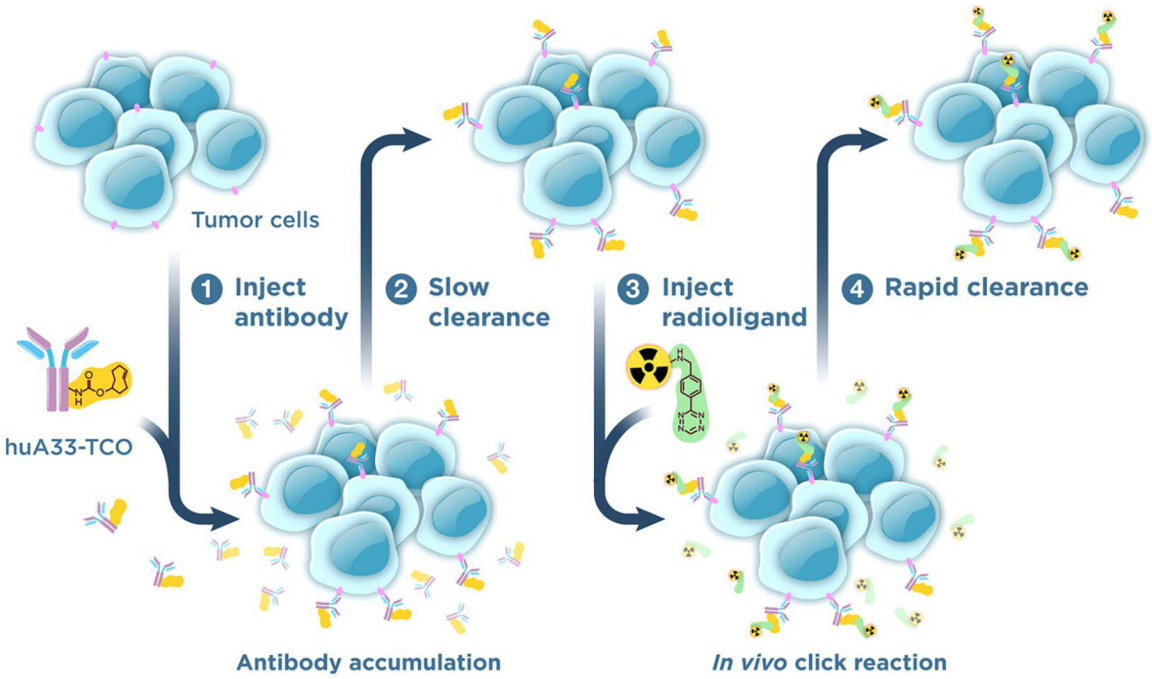

Figure 1.

Schematic of pretargeting using the inverse electron demand Diels-Alder reaction between a TCO-labeled antibody and a radiolabeled tetrazine. Reproduced with permission from reference 6.

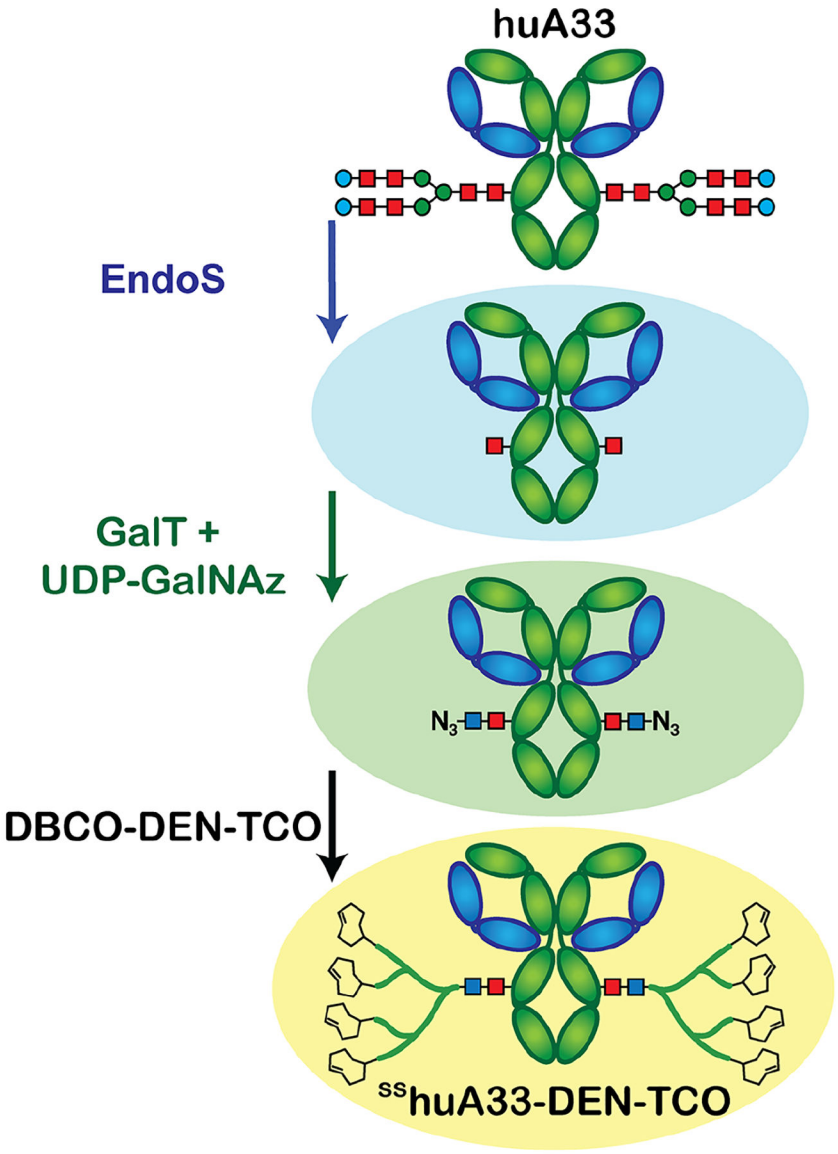

Figure 2.
Chemoenzymatic strategy for the site-specific labeling of antibodies using EndoS

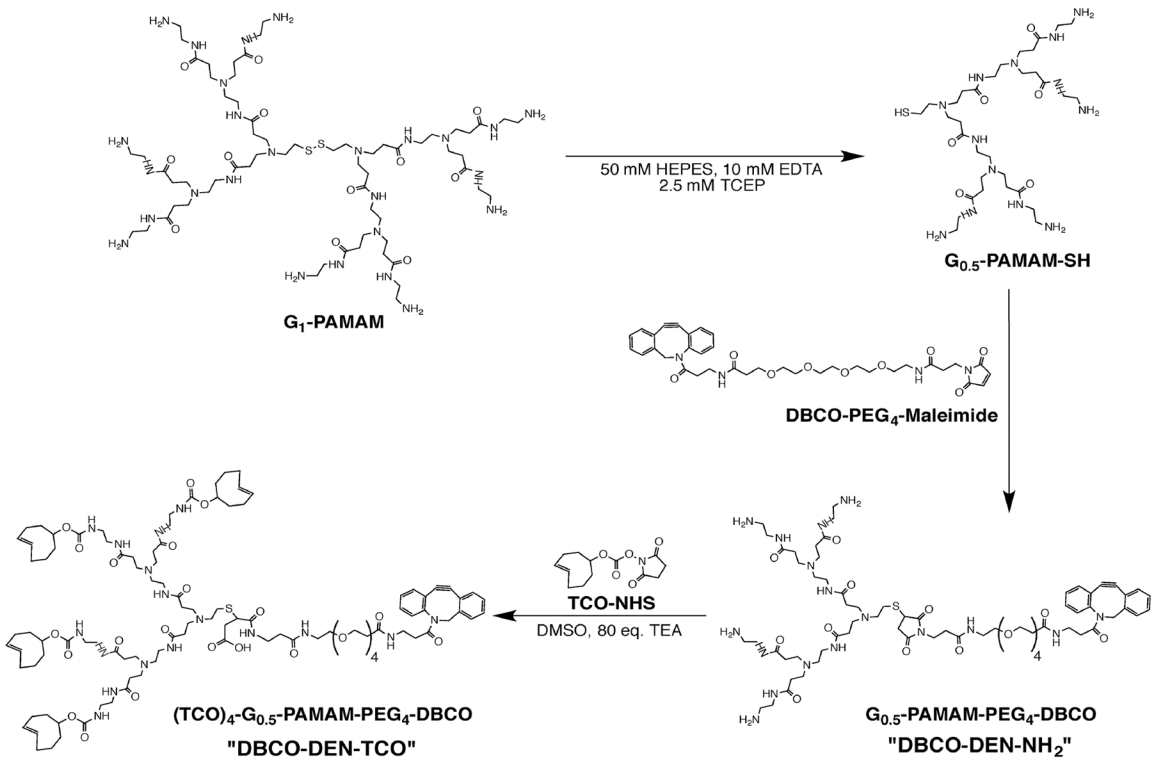

Figure 3.
Synthesis of the TCO-bearing PAMAM dendrimer (DBCO-DEN-TCO)

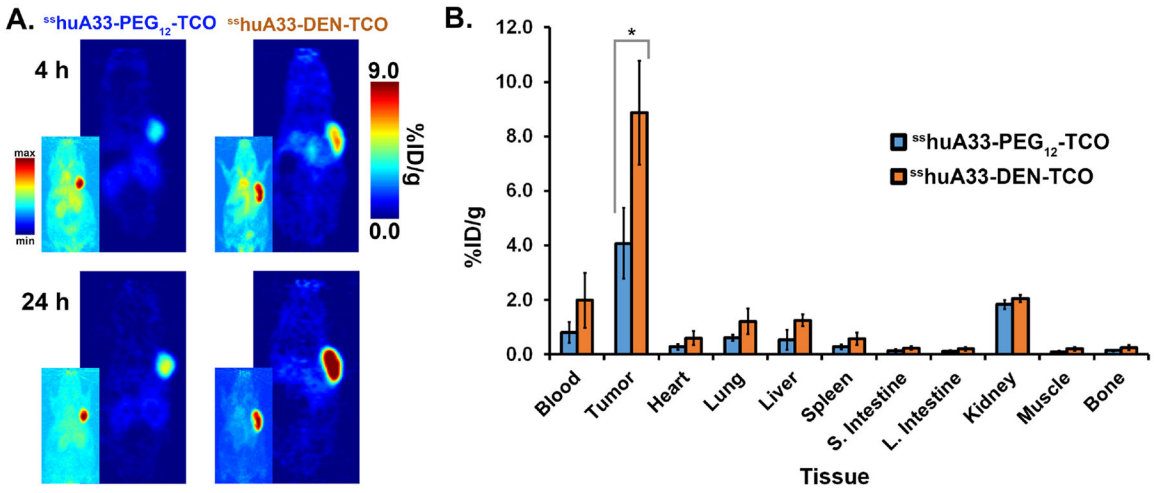

Figure 4.

In vivo pretargeting study in athymic nude mice (n = 4) bearing subcutaneous SW1222 xenografts on their right shoulder. The mice received 100 μg (0.67 nmol) of either ^{ss}huA33-PEG$_{12}$-TCO or ^{ss}huA33-DEN-TCO followed 120 h later by the injection of [^{64}Cu]Cu-SarAr-Tz (16.7 MBq, 0.75 nmol). (A) PET imaging at 4 h (top) and 24 h (bottom) post-injection of radioligand showing clear tumor delineation. Inserts depict maximum intensity projections for each time point. (B) Biodistribution at 24 h after the administration of the radioligand demonstrating significantly higher tumoral activity concentrations in the mice treated with ^{ss}huA33-DEN-TCO. *P<0.05.

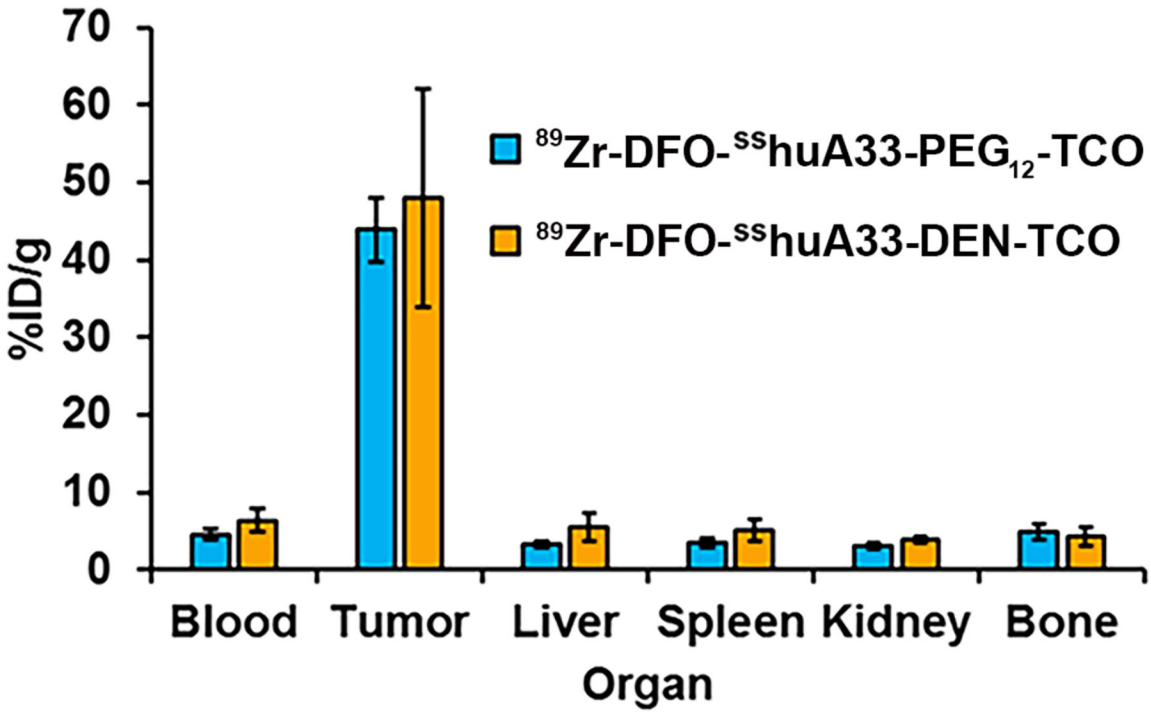

Figure 5.

Biodistribution of 89Zr-DFO-^{ss}huA33-DEN-TCO and 89Zr-DFO-^{ss}huA33-PEG$_{12}$-TCO in athymic nude mice (n = 5) bearing subcutaneous SW1222 xenografts. Cohorts were administered 100 μg of either radioimmunoconjugate and sacrificed 120 h later.

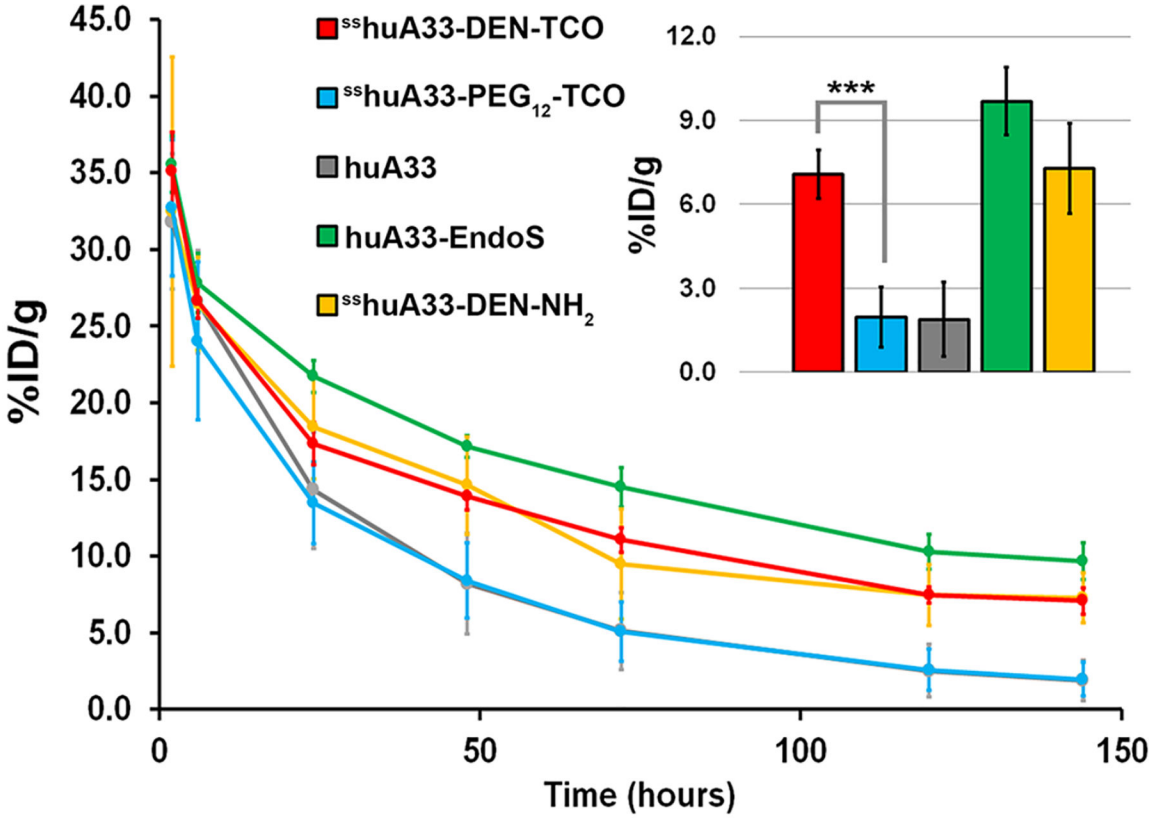

Figure 6.

Blood clearance curves for the various ^{89}Zr-DFO-labeled huA33 immunoconjugates. Insert shows final blood values at 144 h in % ID/g (***P<0.0005).